HEAT TRANSFER IN INHOMOGENEOUS DISPERSED SYSTEMS BASED ON GRAPHENE OXIDE HYDROGELS

Boris POKUSAEV[1,2,*], Andrey MOSHIN[1,2], Dmitry NEKRASOV[1,2], Dmitry KHRAMTSOV[2], Nicolay ZAKHAROV[2] and Raphael KHAIROV[1]

[1]Moscow Polytechnic University, Moscow, Russia
[2]MIREA – Russian Technological University, Moscow, Russia
[*] Corresponding author; E-mail: pokusaev2005@yandex.ru

Based on the optical holography method, studies of the occurrence and development of convective flows in hydrogels of various concentrations with the addition of graphene oxide in relation to 3D-bioprinting technology have been performed. For quantitative measurement of temperature fields, the optical holography method was used in combination with the gradient thermometry method, based on the dependence of the refractive index on the properties of hydrogel systems modified with graphene oxide with different concentrations and temperatures. Under conditions of changes in the thermophysical properties of hydrogels, as well as the magnitude of the supplied heat flux, the features of heating the wall area are studied in order to determine the coefficients of thermal conductivity and heat capacity, as well as the nature of the formation of convective flows near the wall heated from below.
Keywords: *hydrogels, 3-D bioprinting, thermophysical properties of hydrogels, graphene oxide, gradient thermometry.*

1. Introduction

Currently area of regenerative technology and bioprinting is actively developing. These technologies cannot be developed without the parallel creation of a new cluster of materials, and these are mainly hydrogels, which not only create favorable conditions for a wide range of cell cultures, but also allow controlling of their properties. At the same time, the range of such properties is so wide, and the need for their combinations is so diverse that the study of their dependencies on a large number of factors becomes a separate field of research to which a number of works are devoted aimed at studying properties, creating methods for their diagnosis and technologies for their production [1-4] and their number is only growing.

Today, there is also a tendency to create bioinks modified by various components on different bases, the addition of which, even in very low concentrations, can significantly affect both the structure and properties of the main, in particular hydrogel, composition. One of these components is graphene in its various variants. The study of its effect on a wide range of materials has been carried out for quite a long time and continues, in particular, in the form of an analysis of the mechanical and chemical properties of composites and polymers with graphene additives in relation, among other things, to additive technologies [5-7]. Recent advances in the use of this material in relation to technologies for creating modified bioinks and technologies for working with them are described in [8]. This paper describes both various types of graphene-based materials and their application options to achieve the

specified properties of bioinks. It is also worth noting the highlighted areas of research on the effect of graphene and its derivatives, which can be divided into several independent sections such as: analysis of the effect on structure and rheology [9-11], the effect on thermal and electrical properties [12], as well as biocompatibility and manufacturability [13,14]. At the same time, it should also be noted that the list of graphene-based materials, as well as the sizes and form factors of the particles planned for use, are quite extensive, which further complicates both the application of various diagnostic techniques for such systems and the generalization of experimental and calculated data. For example, the particles of graphene, as a material consisting of two-dimensional hexagonal layers of sp2-hybridized carbon atoms forming layered structures with a clear geometry [15], despite the relative chemical inertia along the surface, still have activity with various chemical groups, which must be taken into account when using them. The use of graphene oxide obtained in various ways, such as [16] or [17], is also of interest. Graphene oxide particles have increased mechanical strength, can be manufactured in various form factors and size groups, which also makes this material suitable for various applications in tissue engineering [18,19]. There are also several other modifications, for example, Reduced Graphene Oxide and especially Functionalized Graphene Oxide, which are of particular interest for the engineering of bone and cartilage tissues, which was shown in [20,21].

However, despite the growing number of studies, large gaps remain regarding both the methods of studying the properties of hydrogel and other materials modified by graphene-based components, as well as the dependencies of the properties themselves on various types, form factors and concentrations of the modifying component. At the same time, if the number of works on the study of electrically conductive [22,23] and mechanical properties [24,25], as well as biocompatibility [26,27] is quite high, then issues related to the study of thermal and mass-conducting properties are considered much less often, which does not negate their importance.

Thus, the issue of determining the thermophysical and mass-transfer properties of modified hydrogel materials, as well as the creation of reliable calculation methods for modeling heat and mass transfer processes in such systems is of high importance. The purpose of this work is to implement an experimental complex for non-contact diagnostics of temperature fields and heat fluxes during non-stationary heating of hydrogel materials with the addition of graphene oxide, which allows determining their thermophysical properties.

2. Experimental setup and measurement methodology

In experiments investigating heat exchange processes in hydrogel materials with the addition of graphene oxide of different concentrations, which were accompanied by phase transitions, the previously described [28] method of holographic interferometry in combination with gradient thermometry was used. This method provides high sensitivity and accuracy of measurements.

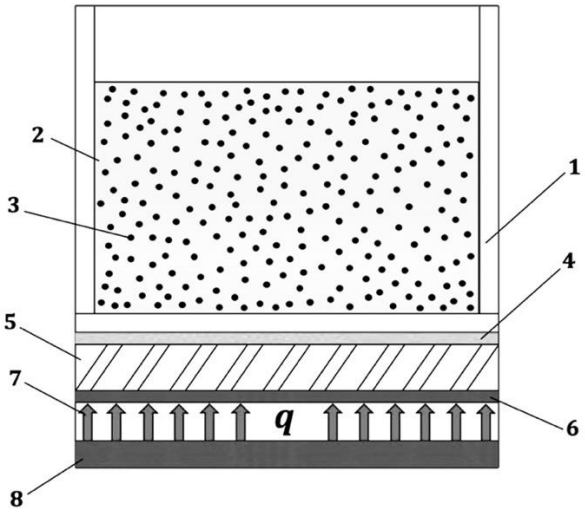

Figure 1. Diagram of the working area: *1 – optical cell, 2 – hydrogel, 3 – graphene oxide, 4 – thermal paste, 5 – gradient heat flow sensor, 6 – electrical insulation layer, 7 – heater, 8 – thermal insulation.*

The research was carried out on an experimental stand for measuring temperature fields in hydrogel materials based on agarose and gelatin with the addition of graphene oxide. Figure 1 schematically shows the experimental section, which includes a transparent cuvette (*1*) with dimensions of 5 x 10 *mm* and a height of 15 *mm*, which was filled with the studied microstructured medium based on pure and combined agarose-gelatin hydrogels (*2*) and graphene oxide, the concentration of which varied from 0.1% to 1% by weight (*3*). A gradient heat flow sensor (*5*) is mounted in the lower part of the cuvette, a layer of thermal paste (*4*), an electrical insulation layer based on technical mica with a thickness of 0.05 *mm* (*6*), thermal insulation made of textolite (*8*) and an electric heater (*7*), with which heat was supplied with a controlled supply of thermal load power. The heating power varied in the range from 1.5-3.5 *W*.

3. Visualization and study of the distribution of temperature fields in hydrogels with the addition of graphene oxide

Based on high-speed video recording of unsteady heating of hydrogels with the addition of graphene oxide (0.1% by weight) Interference patterns of the process under study were obtained.

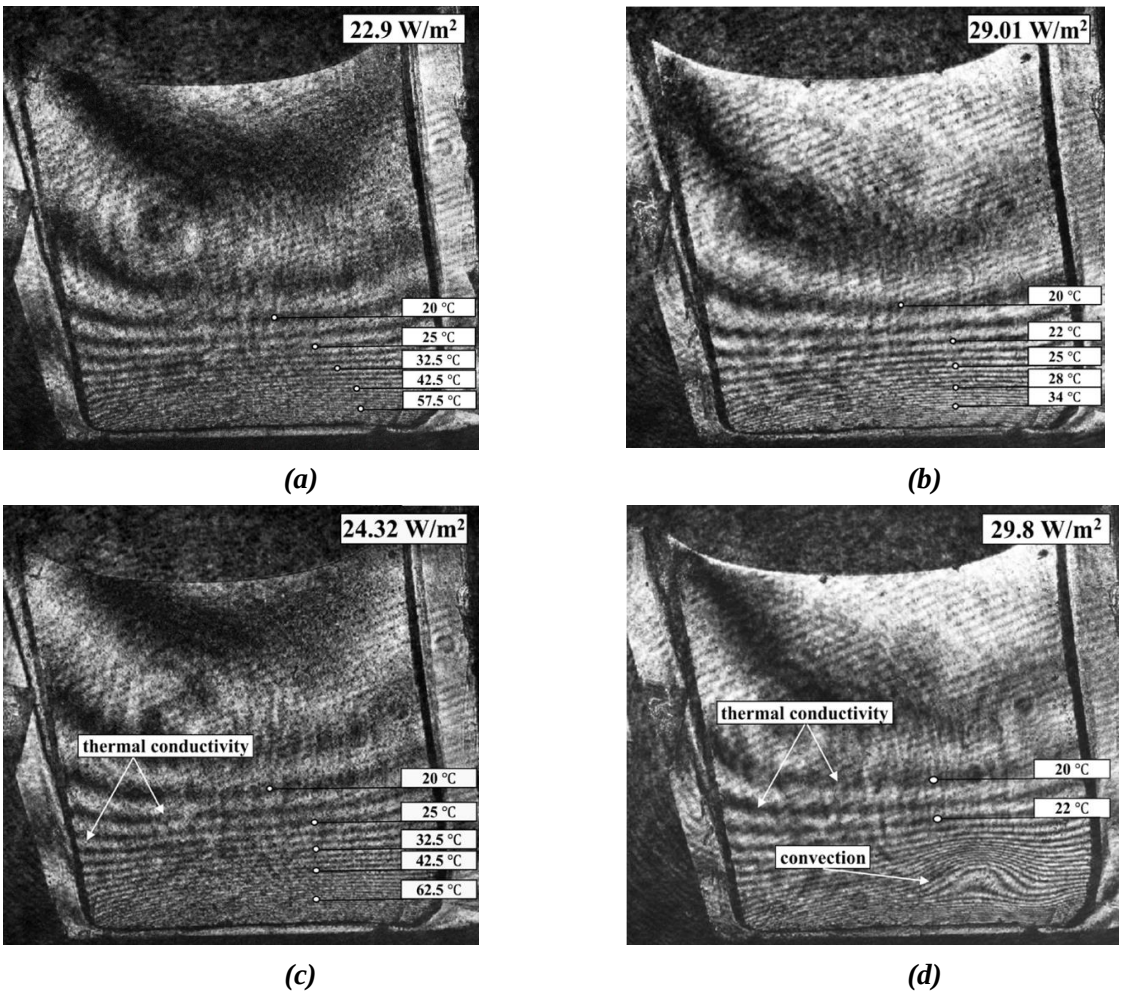

Figure 2. Video frames of temperature fields for different hydrogel samples at the same time τ =20 c from the start of heating (a,b), τ =25 c (c,d) at N = 1.5 W: *a) agarose gel 0.4% by weight and graphene oxide 0.1% by weight, b) gelatin gel 0.4% by weight and graphene oxide 0.1% by weight, c) agarose gel 0.4% by weight and graphene oxide 0.1% by weight, d) gelatin gel 0.4% by weight and graphene oxide 0.1% by weight.*

As an example, Fig.2 (*a,b*) shows video frames of measuring temperature fields after 20 seconds, Fig. 2 (*c,d*) – 25 seconds from the start of heating. Here, a scale with the restored values of the temperature fields for agarose and gelatin gels with the addition of graphene oxide is shown. The thermal load installed on the current source was $N = 1.5\ W$. The isotherms shown in Fig. 2 (*a,b*), parallel to the heating surface, characterize the mode of classical unsteady thermal conductivity. As can be seen from Fig. 2 (*c,d*), in the case of gelatin gel Fig. 2 (*d*) at a characteristic time of 25 seconds, a phase transition occurs, a convective flow is realized, while in the agarose gel Fig. 2 (*c*) a mode of non-stationary thermal conductivity is observed. Here, the estimated error of optical measurements, which depends on the resolution of the photosensitive element of the video camera and the depth of the working area along the light beam ($L = 5\ mm$), did not exceed 5%.

To get numerical values the temperature dependences of the refractive index were determined for various samples of both pure and mixed hydrogel, which contains 0.1% graphene oxide. Fig. 3 shows the characteristic dependences of the refractive index for two pure gels and one mixed at the wavelength of

the *He-Ne* laser. As can be seen from the figure, the dependence of the refractive index in this temperature range is significant.

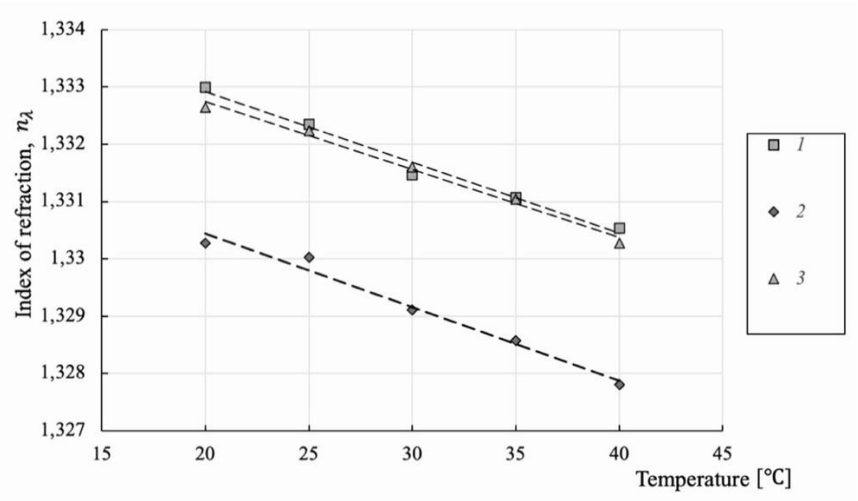

Figure 3. Dependence of the refractive index for different gels on the temperature at the wavelength λ = 632.8 nm: *1 – gelatin gel 4.0% by weight, 2 – agarose gel 0.4% by weight, 3 – mixed gel of agarose and gelatin, respectively 0.1% and 4.0% by weight; points are experimental data, lines are calculated values.*

As can be seen in Fig. 3, the refractive indices for pure gelatin and mixed hydrogel with the addition of graphene oxide Fig. 3 (*1,3*) practically do not differ in this temperature range, but their values are significantly higher than the data with agarose gel Fig. 3 (*2*). Using these approximation dependences of refractive indices on temperature, the values were calculated temperature gradients for both pure and mixed gel samples. These data make it possible to further determine the coefficients of thermal conductivity and heat capacity for hydrogel materials modified with graphene oxide.

Using the implemented technique [29], characteristic, temperature differences were obtained for both pure gelatin and agarose and mixed hydrogels (with graphene oxide 0.1% by weight), which amounted to ΔT = 1 °C, 1.6°C and 2.5°C, respectively. These data allow us to obtain temperature values at any point of the test sample in time, which are necessary to solve the inverse problem of thermal conductivity and determine the calculated values of heat transfer coefficients.

4. Influence of graphene oxide concentration on the time of occurrence of convective flows in hydrogel materials

Fig. 4,6,8 show video footage of the moment of the onset of convection in pure agarose, gelatin and mixed gel in the presence of graphene oxide in different concentrations. The experiments were performed at a heater power of N = 3.5 *W*.

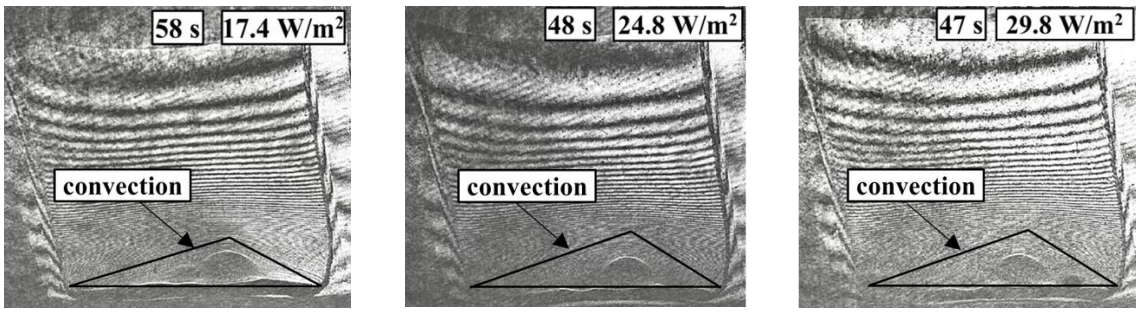

(a) *(b)* *(c)*

Figure 4. Interference patterns of convection in a hydrogel cell at power N = 3.5 W at different time points: *a) agarose gel 0.4% by weight, b) agarose gel 0.4% by weight and graphene oxide 0.1% by weight, c) agarose gel 0.4% by weight and graphene oxide 1% by weight.*

As can be seen, with an increase in the concentration of graphene oxide, the density of the heat flux increases, and this in turn leads to a decrease in the generation time of convective flows. A special feature of experimental studies of unsteady heat transfer in inhomogeneous microstructures hydrogels was a combination of optical and thermometric methods. The use of a gradient heat flow sensor makes it possible to record the dynamics of changes in the magnitude of the surface heat flow over time and synchronize it with the results of high-speed video recording of the process of unsteady heating of hydrogel samples.

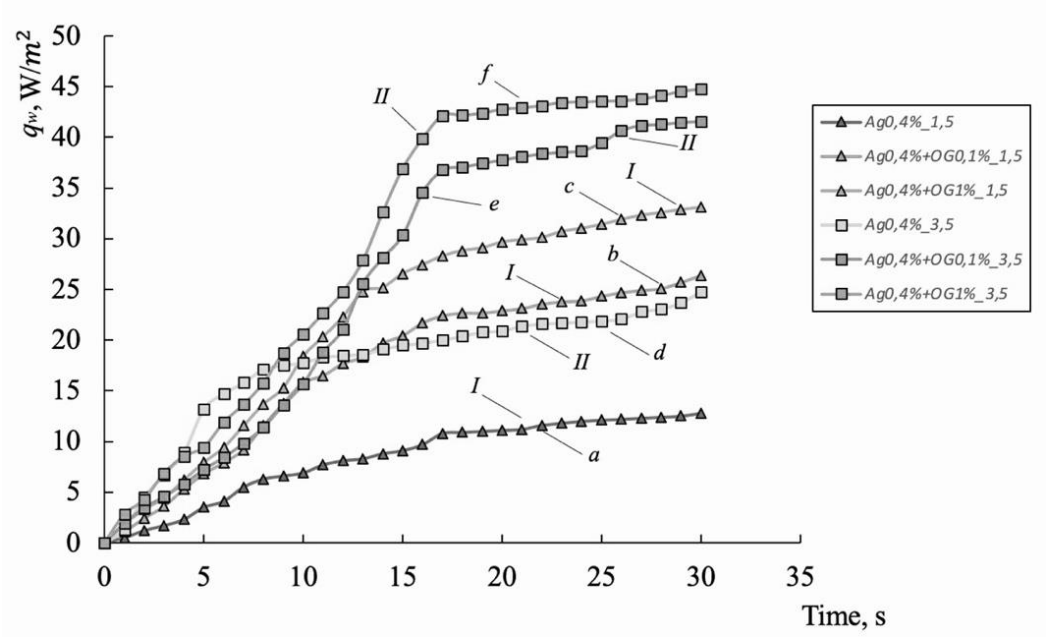

Figure 5. Changes in the heat flow density q_w (W/m²) from time under different modes of heat load in the heater: *I – at 1.5W, a) agarose gel 0,4 % by weight, b) agarose gel 0,4 % by weight and graphene oxide 0,1% by weight, c) agarose gel 0,4 % by weight and graphene oxide 1% by weight; II – at 3.5W, d) agarose gel 0,4 % by weight, e) agarose gel 0,4 % by weight and graphene oxide 0,1% by weight, f) agarose gel 0,4 % by weight and graphene oxide 1% by weight.*

Fig. 5,7,9 shows the experimental results of measuring the density of the surface heat flux in the area of the lower wall of the cell at a given power N = 1.5 and 3.5 W for both pure hydrogels and with the

addition of graphene oxide of different concentrations. The graphs show that with an increase in the concentration of graphene oxide, the heat fluxes for all the studied hydrogels increase. In the case of a mixed gel, the features of the behavior of the heat flow over time for N = 1.5 and 3.5 W Fig. 9 (c,e). They are apparently related to the patterns of the phase transition of such gels. The data obtained are important for the creation and verification of computational methods for solving the problem of the spatiotemporal distribution of temperature fields in gels with the addition of graphene oxide, including the possibility of predicting the onset of melting and the occurrence of microconvective flows.

Further, Fig. 6 and 8 show interference patterns of convection in a hydrogel cell at power N=3.5 W at different time points for gelatin and mixed hydrogel samples.

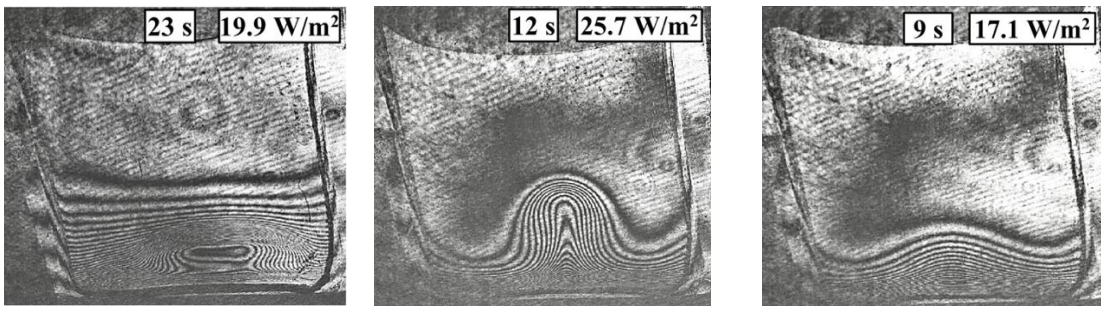

(a) *(b)* *(c)*

Figure 6. Interference patterns of convection in a hydrogel cell at power N = 3.5 W at different time points: *a) gelatin gel 4% by weight, b) gelatin gel 4% by weight and graphene oxide 0.1% by weight, c) gelatin gel 0.4% by weight and graphene oxide 1% by weight.*

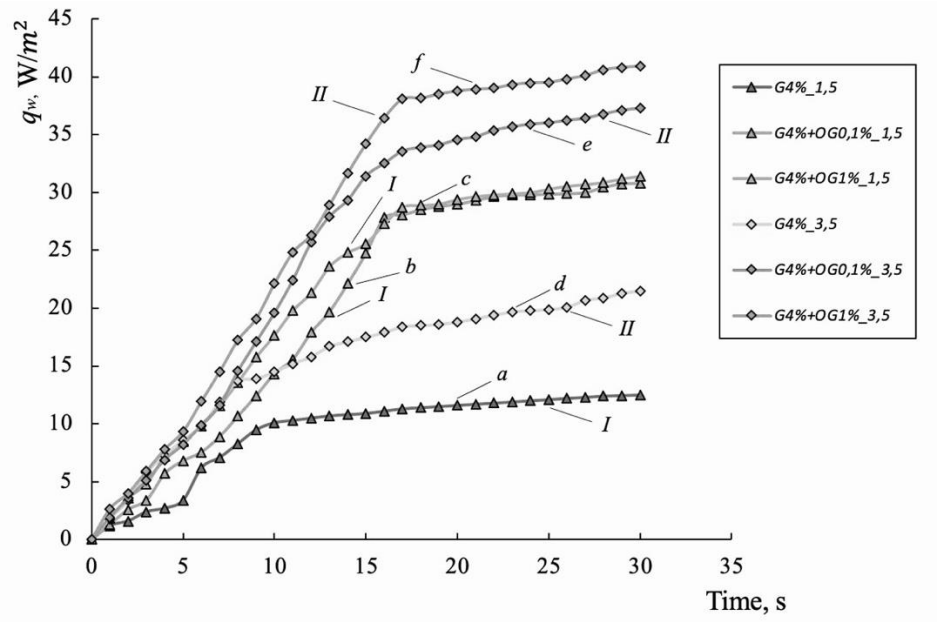

Figure 6. Changes in the heat flow density q_w (W/m^2) from time under different modes of heat load in the heater: *I – at 1.5W, a) gelatin gel 4 % by weight, b) gelatin gel 0,4 % by weight and graphene oxide 0,1% by weight, c) gelatin gel 4 % by weight and graphene oxide 1% by weight;*
II – at 3.5W, d) gelatin gel 4 % by weight, e) gelatin gel 4 % by weight and graphene oxide 0,1% by weight, f) gelatin gel 0,4 % by weight and graphene oxide 1% by weight.

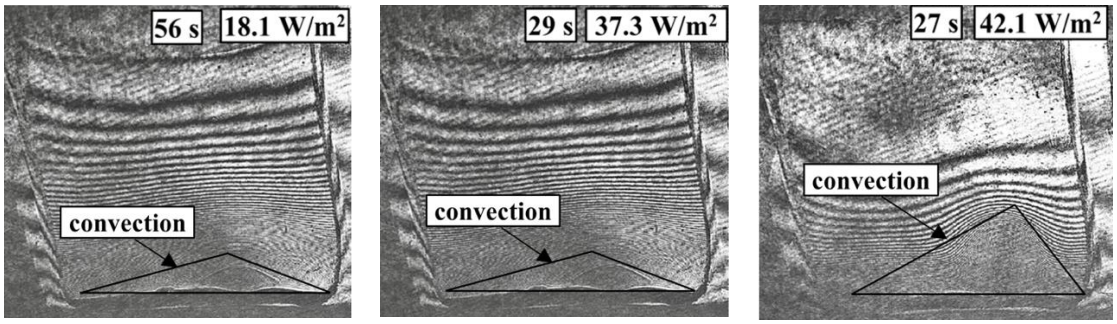

(a) *(b)* *(c)*

Figure 8. Interference patterns of convection in a hydrogel cell at power N = 3.5 W at different time points:

a) mixed gel of agarose 0.1% by weight and gelatin 4.0% by weight, b) mixed gel of agarose 0.1% by weight, gelatin 4.0% by weight and graphene oxide 0.1% by weight,

c) mixed gel of agarose 0.1% by weight, gelatin 4.0% by weight and graphene oxide 0.1% by weight.

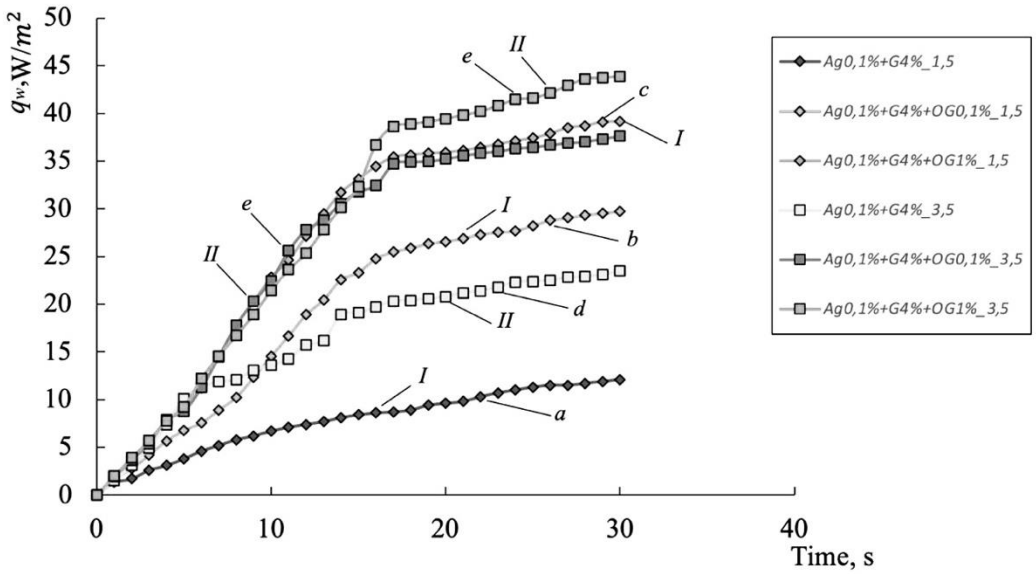

Figure 9. Changes in the heat flow density q_w (W/m²) from time under different modes of heat load in the heater: *I – at 1.5W, a) mixed gel of agarose 0.1% by weight and gelatin 4.0% by weight, b) mixed gel of agarose 0.1% by weight, gelatin 4.0% by weight and graphene oxide 0.1% by weight, c) mixed gel of agarose 0.1% by weight, gelatin 4.0% by weight and graphene oxide 1% by weight,*

II – at 3,5 W, d) mixed gel of agarose 0.1% by weight and gelatin 4.0% by weight,

e) mixed gel of agarose 0.1% by weight, gelatin 4.0% by weight and graphene oxide 0.1% by weight,

f) mixed gel of agarose 0.1% by weight, gelatin 4.0% by weight and graphene oxide 0.1% by weight.

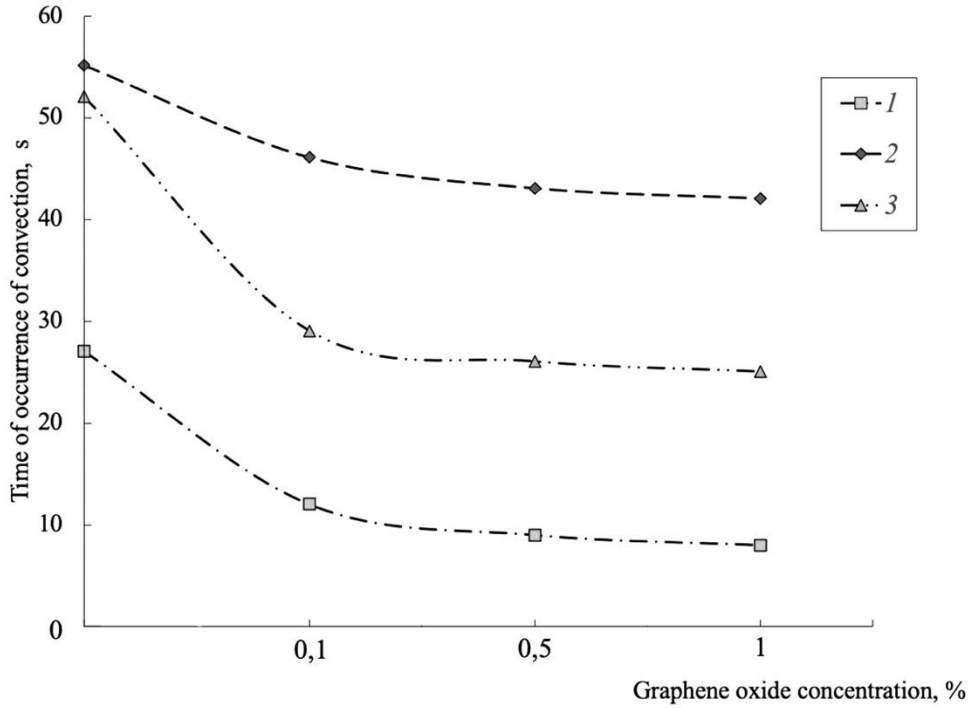

Figure 10. Dependence of the time of occurrence of convective flows in hydrogels on the concentration of graphene oxide at a heat dissipation power *at 3.5W: 1 – gelatin gel 4.0% by weight, 2 – agarose gel 0.4% by weight, 3 – mixed gel of agarose and gelatin, respectively 0.1% and 4.0% by weight.*

Fig. 10 shows the results of the dependence of the time of occurrence of convective flows in hydrogels on the concentration of graphene oxide at a characteristic heat dissipation power of 3.5 *W*. From which it can be seen that the addition of graphene oxide, even in a very small concentration, leads to a significant change in thermophysical properties, and therefore the time of convection.

6. Numerical modeling

To determine the thermophysical properties, a physical and mathematical formulation of the one-dimensional problem of thermal conductivity in a Cartesian coordinate system was formulated:

$$C\frac{\partial T}{\partial t} = \lambda\frac{\partial^2 T}{\partial x^2}, t > 0, 0 < x < L; \quad (1)$$

$$T(x,0) = T_0; \quad (2)$$

$$-\lambda\frac{\partial T(0,t)}{\partial x} = q(t); \quad (3)$$

$$\frac{\partial T(X,t)}{\partial x} = 0; \quad (4)$$

Determining the coefficients C and λ according to known experimental temperature values $T(x_m, \tau_n)$ at points in time τ_n at the points of the material sample x_m it is the essence of the coefficient inverse problem of thermal conductivity. One of the methods for solving inverse problems of thermal conductivity is the integral representation of the solution, when the desired coefficients of the differential equation are written as a set of integrals of temperature and heat flow.

A feature of the method is the introduction of a weight function *p(x)* [30], the variation of which allows you to explicitly express the thermal conductivity, without dependence on the heat capacity. The method allows you to bring the differential equation modeling the process to an equivalent integral

equation. If we put a weight function in the integral equation, p = 1, then we get the equation for determining the volumetric heat capacity C regardless of thermal conductivity λ.

$$C = \frac{q(t)}{\frac{d}{dt}\int_0^L T(x,t)dx} \quad (5)$$

Similarly, putting the weight function into the integral equation $p = x$, we obtain a calculation formula for determining the thermal conductivity:

$$\lambda = \frac{C*\frac{d}{dt}\int_0^L x*T(x,t)dx}{T_0(t)-T_L(t)} \quad (6)$$

The numerical solution was implemented in Python version 3.10.5. The values of the thermal conductivity and volumetric heat capacity coefficients obtained from the calculations are presented below:

Table 1. Calculated values of thermal conductivity and heat capacity of hydrogel material

Substance type	λ, [$Wm^{-1}K^{-1}$]	C, [$kJm^{-3}K^{-1}$]
Gelatin gel 4% and graphene oxide 0,1%	0,545	2367
Agarose gel 0,4 % and graphene oxide 0,1%	0,569	2386

Thanks to the computational and experimental complex, it is possible to achieve high accuracy in determining the thermophysical characteristics of hydrogel materials modified with graphene oxide. This makes it possible to use these techniques to quickly analyze the properties of promising bioinks based on them at various concentrations.

7. Conclusions

New data on the reduced temperature fields in hydrogel materials modified with graphene oxide have been obtained. The application of the gradient thermometry method made it possible to observe changes in the heat flow on the surface over time and correlate them with the data of high-speed video recording of the heating process of hydrogel samples. Quantitative values of the temperature difference between two interference bands of the studied samples of gel materials with the addition of graphene oxide were obtained. Using the implemented technique, characteristic temperature differences were obtained for both pure gelatin and agarose and mixed hydrogels (with graphene oxide 0.1% by weight), which amounted to ΔT = 1 °C, 1.6 °C and 2.5 °C, respectively. It was found that with an increase in the concentration of graphene oxide, the heat fluxes for all the studied hydrogels increase. In the case of a mixed gel, the features of the behavior of the heat flow over time for N = 1.5 and 3.5W are apparently related to the patterns of the phase transition of such gels. Thus, graphene oxide, present even in such insignificant concentrations, has a significant effect on the thermophysical properties of hydrogel materials and can be used to modify them in 3D bioprinting technologies. Therefore, when adding graphene-based components, it is necessary to be careful and investigate their effect on the base in the complex, since, for example, by giving electrically conductive properties to the main gel material, we simultaneously change the thermophysical properties, which in turn will certainly affect the technological modes in the printing device.

Acknowledgment

This study was conducted with the financial support of the Moscow Polytechnic University within the framework of the V.E. Fortov grant. The team of authors expresses appreciation to Department of Low Temperatures of the National Research University of the Moscow Power Engineering Institute for providing a sample of graphene oxide for conducting experiments.

Nomenclature

C – heat capacity coefficient, [kJm^{-3} K^{-1}]

GO – graphene oxide

N – power, [W]

p – weight function

t – time, [s]

$q(t)$ – heat flow density, [W/m^2]

T_0 – initial temperature, [°C]

x – coordinate, [m]

Greek symbols

λ - thermal conductivity coefficient, [$Wm^{-1}K^{-1}$]

τ – time, [s]

References

[1] Xu, W., *et al*., 3D printing enabled nanoparticle alignment: A review of mechanisms and applications. Small: Year 2021, *17*, 2100817.

[2] Kumar, V., *et al*., Drug delivery and testing via 3D printing, *Bioprinting, 36* (2023), 00298.

[3] Banga, H., *et al*., Design and fabrication of prosthetic and orthotic product by 3D printing. In Prosthetics and Orthotics; IntechOpen: London, UK, 2020.

[4] Pokusaev, B., *et al*., The Effect of Bioresorbable Additives and Micro-Bioobjects on gel formation, stabilization and thermophysical properties. *Thermal Science*, *23* (2019), 2B, pp. 1297-1310.

[5] Itapu, B., *et al*., A review in graphene/polymer composites, *Chem. Sci. Int. J.*, *23* (2018), pp. 1–16.

[6] Palmieri, V., *et al*., Graphene-based scaffolds for tissue engineering and photothermal therapy. *Nanomedicine*, *15* (2020), pp. 1411–1417.

[7] Mantecón-Oria, *et al*., Influence of the properties of different graphene-based nanomaterials dispersed in polycaprolactone membranes on astrocytic differentiation, *Sci. Rep*., *12* (2022), 13408.

[8] Patil, R., *et al*., Graphene in 3D Bioprinting. *J. Funct. Biomater*. *15* (2024), 82, pp. 1 – 21.

[9] Hong, N., *et al*., 3D Bioprinting and Its in vivo Applications. *J. Biomed. Mater. Res*., Part B *106* (2018), 1, pp. 444−459.

[10] Holzl, K., *et al*., Bioink Properties Before, During and After 3D Bioprinting, *Biofabrication, 8* (2016), 3, 032002.

[11] Gillies, A., *et al*., Structure and Function of the Skeletal Muscle Extracellular Matrix, *Muscle Nerve, 44* (2011), 3, pp. 318−331.

[12] Derakhshanfar, S., *et al*., 3D Bioprinting for Biomedical Devices and Tissue Engineering: A Review of Recent Trends and Advances, *Bioact. Mater*., *3* (2018), 2, pp. 144−156.

[13] Shi, Y., *et al*., Tyrosinase-doped Bioink for 3D Bioprinting of Living Skin Constructs, *Biomed. Mater*, *13* (2018), 3, 035008.

[14] Haring, A., *et al*., Process and Bio-inspired Hydrogels for 3D Bioprinting of Soft Free-standing Neural and Glial Tissues, *Biofabrication*, *11* (2019), 2, 025009.

[15] Birenboim, M., *et al*., Reinforcement and workability aspects of graphene-oxide-reinforced cement nanocomposites. *Compos. Part. B Eng*. *161* (2019), pp. 68–76.

[16] Yoo, M., *et al*., Effect of hydrogen peroxide on properties of graphene oxide in Hummers method, *Carbon* 141 (2019), pp. 515–522.

[17] Dmitriev, A., *et al*., Prospects for the Use of Two-Dimensional Nanomaterials in Energy Technologies (Review), *Thermal Engineering*, *70* (2023), 8, pp. 551-572.

[18] Motiee, S., *et al*., Investigation of physical, mechanical and biological properties of polyhydroxybutyrate-chitosan/graphene oxide nanocomposite scaffolds for bone tissue engineering applications, *Int. J. Biol.Macromol*., *247* (2023), 125593.

[19] Challa, A., *et al*., Graphene oxide produced from spent coffee grounds in electrospun cellulose acetate scaffolds for tissue engineering applications, *Mater Today Commun*, *35* (2023), 105974.

[20] Wajahat, M., *et al*., 3D printing of Fe3O4 functionalized graphene-polymer (FGP) composite microarchitectures, *Carbon*, *167* (2020), pp. 278–284.

[21] Palaganas, J., *et al*., 3D printing of covalent functionalized graphene oxide nanocomposite via stereolithography, *ACS Appl. Mater. Interfaces*, *11* (2019), pp. 46034–46043.

[22] Ibrahim, A., *et al*., Graphene-based nanocomposites: Synthesis, mechanical properties, and characterizations, *Polymers*, *13* (2021), 2869.

[23] Vatani, M., *et al*., Simulating of effective conductivity for graphene–polymer nanocomposites, *Sci. Rep*.13 (2023), 5907.

[24] Haney, R., *et al*., Printability and performance of 3D conductive graphite structures, *Addit. Manuf*., *37* (2021), 101618.

[25] Borode, A.., *et al*., Effect of various surfactants on the viscosity, thermal and electrical conductivity of graphene nanoplatelets Nanofluid, *Int. J. Thermophys*, *42* (2021), 158.

[26] Solìs Moré, *et al*., Biocompatibility of composites based on chitosan, apatite, and graphene oxide for tissue applications, *J. Biomed. Mater. Res*. Part A 106 (2018), 106, pp. 1585–1594.

[27] Patil, R., *et al*., Dispersed graphene materials of biomedical interest and their toxicological consequences, *Adv. Colloid Interface Sci.* 2020, 275, 102051.

[28] Zakharov, N. S., *et al*., Research of Heat Transfer Processes in Hydrogels by Holographic Interferometry and Gradient Thermometry (in Russian), Technical Physics Letters, 48 (2022), 9, pp. 10-14.

[29] Pokusaev, B., *et al*., Study of Hydrogel Materials Thermophysical Properties, *Thermal Science, 27* (2023), 27, 5A, pp. 3701-3708.

[30] Dmitriev, O. S., et al., Numerical-Analytical Solution of the Nonlinear Coefficient Inverse Heat Conduction Problem (in Russia)., Journal of Engineering Physics and Thermophysics, 91 (2018), 6, pp. 1353–1364.

Submitted: 24.01.2024.
Revised: 20.04.2024.
Accepted: 03.05.2024.